

Polyimide-Side-Chain Tethered Polyhedral Oligomeric Silsesquioxane Nanocomposites for Low-Dielectric Film Applications

Chyi-Ming Leu, Yao-Te Chang, and Kung-Hwa Wei*

Department of Materials Science and Engineering, National Chiao Tung University, Hsinchu, Taiwan 30049 R.O.C.

Received May 14, 2003. Revised Manuscript Received July 17, 2003

Low-dielectric-constant nanoporous films (dielectric constant, $k = 2.4$) with thermal integrity and controllable mechanical strength have been prepared by covalently tethering nanoporous polyhedral oligomeric silsesquioxane (POSS) molecules, 1-nm size, to the side chains of polyimide. The tethered POSS molecules in the amorphous polyimide retain a nanoporous crystal structure, but form an additional ordered architecture due to microphase separation. With this approach, the dielectric constant of the film can be tuned by the amount of POSS molecules introduced in the nanocomposite film; the polyimide molecules offer additional advantages of maintaining certain thermal and mechanical strengths.

Introduction

The demand for low-dielectric-constant (low- k) materials in the microelectronics industry has recently led to extensive efforts to explore the applicability of porous materials, with a special focus on nanoporous materials.^{1–4} Low- k materials can be prepared by introducing voids into the film to take advantage of the low dielectric constant of air ($k = 1$). Homogeneous, nanometer-sized, closed pores are preferred to preserve the electric and mechanical properties of the material.

Polyimides are well-known for their high-temperature durability (service temperatures can exceed 400 °C) and mechanical strength. Polyimides are used as interlayer dielectrics in microelectronics applications by simple spin-coating techniques.^{5–7} One approach for producing porous, low- k polyimides is based on creating voids by thermal degradation of the poly(propylene oxide) block of a phase-separated polyimide–poly(propylene oxide) block copolymer.^{8,9} In this approach, it is critically important to completely remove the residual organic compound and produce uniform, controllable, and closed pores.

We wonder if, in another approach, preformed and uniform nanoporous inorganic species can be incorporated into polyimide to reduce the dielectric constant

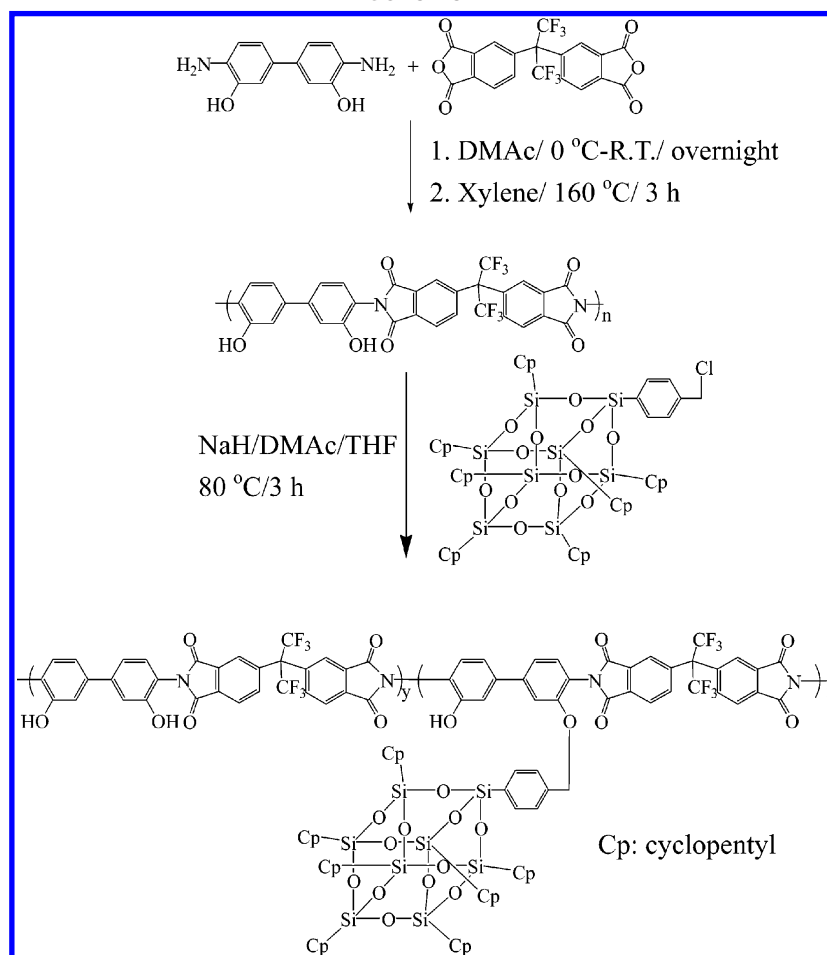
without detrimentally affecting the mechanical properties of the polyimide. For example, one member of the polyhedral oligomeric silsesquioxane (POSS) family, octamer (RSiO_{1.5})₈, which consists of a rigid and cubic silica core with a nanopore about 0.3 to 0.4 nm,¹⁰ is a possible candidate; here, the R group can react with linear or thermosetting polymers.^{10–24} Their incorporation into some polymers has led to enhancements in thermal stability and mechanical properties,^{12,13,16} such as in the case of acrylics,¹¹ styryls,¹³ epoxies,^{14,18,21} and polyethylene.²⁴ One variation of (RSiO_{1.5})₈ is (R₇R'Si₈O₁₂), where R and R' stand for nonreactive and reactive groups, respectively. (R₇R'Si₈O₁₂) is termed POSS in this study. In a previous study, we demonstrated that covalently tethering the nanoporous POSS to the polyimide chain ends results in a material with a lower dielectric constant and controllable mechanical proper-

* To whom correspondence should be addressed. Tel: 886-35-731871. Fax: 886-35-724727. E-mail: khwei@cc.nctu.edu.tw.

- (1) Miller, R. D. *Science* **1999**, *286*, 421.
- (2) Baskaran, S.; Liu, J.; Domansky, K.; Kohler, N.; Li, X. H.; Coyle, C.; Fryxell, G. E.; Thevuthasan, S.; Williford, R. E. *Adv. Mater.* **2000**, *12*, 291.
- (3) Lu, Y. F.; Fan, H. Y.; Doke, N.; Loy, D. A.; Assink, R. A.; LaVan, D. A.; Brinker, C. J. *J. Am. Chem. Soc.* **2000**, *122*, 5258.
- (4) Kresge, C. T.; Leonowicz, M. E.; Roth, W. J.; Vartuli, J. C.; Beck, J. S. *Nature* **1992**, *359*, 710.
- (5) Feger, C.; Franke, H. In *Polyimides Fundamentals and Applications*; Ghosh, M. K., Mittal, K. L., Eds.; Marcel Dekker: New York, 1996; p 7.
- (6) Leu, C. M.; Wu, Z. W.; Wei, K. H. *Chem. Mater.* **2002**, *14*, 3016.
- (7) Jiang, L. Y.; Leu, C. M.; Wei, K. H. *Adv. Mater.* **2002**, *14*, 426.
- (8) Carter, K. R.; DiPietro, R. A.; Sanchez, M. I.; Russell, T. P.; Lakshmanan, P.; McGrath, J. E. *Chem. Mater.* **1997**, *9*, 105.
- (9) Carter, K. R.; DiPietro, R. A.; Sanchez, M. I.; Swanson, S. A. *Chem. Mater.* **2001**, *13*, 213.

- (10) Zhang, C.; Babonneau, F.; Bonhomme, C.; Laine, R. M.; Soles, C. L.; Hristov, H. A.; Yee, A. F. *J. Am. Chem. Soc.* **1998**, *120*, 8380–8391.
- (11) Lichtenhan, J. D.; Vu, N. Q.; Carter, J. A.; Gilman, J. W.; Feher, F. J. *Macromolecules* **1993**, *26*, 2141.
- (12) Lichtenhan, J. D.; Otonari, Y. A.; Carr, M. J. *Macromolecules* **1995**, *28*, 8435.
- (13) Haddad, T. S.; Lichtenhan, J. D. *Macromolecules* **1996**, *29*, 7302.
- (14) Lee, A.; Lichtenhan, J. D. *Macromolecules* **1970**, *31*, 4970.
- (15) Feher, F. J.; Soulivong, D.; Eklud, A. G.; Wyndham, K. D. *Chem. Commun.* **1997**, 1185.
- (16) Fu, B. X.; Zhang, W. H.; Hsiao, B. S.; Rafailovich, M.; Sokolov, J.; Sauer, B. B.; Phillips, S.; Blanski, R. *High Perform. Polym.* **2000**, *12*, 565.
- (17) Jeon, H. G.; Mather, P. T.; Haddad, T. S. *Polym. Int.* **2000**, *49*, 453.
- (18) Haddad, T. S.; Mather, P. T.; Jeon, H. G.; Romo-Uribe, A.; Farris, R.; Lichtenhan, J. D. In *Organic/Inorganic Hybrid Materials*; Laine, R. M., Sanchez, Brinker, Giannelis, Eds.; MRS Symp. Ser. 519; Materials Research Society: Warrendale, PA, 1998; pp 381–386.
- (19) Gilman, J. W.; Schlitzere, D. S.; Lichtenhan, J. D. *J. Appl. Polym. Sci.* **1996**, *60*, 591.
- (20) Gonzalez, R. I.; Phillips, S. H.; Hoflund, G. B. *J. Spacecr. Rockets* **2000B**, *37*, 463.
- (21) Laine, R. M.; Choi, J.; Lee, I. *Adv. Mater.* **2001**, *13*, 800.
- (22) Zhang, C.; Laine, R. M. *J. Am. Chem. Soc.* **2000**, *122*, 6979.
- (23) Tamaki, R.; Tanaka, Y.; Asuncion, M. Z.; Choi, J.; Laine, R. M. *J. Am. Chem. Soc.* **2001**, *123*, 12416.
- (24) Zheng, L.; Waddon, A. J.; Farris, R. J.; Coughlin, E. B. *Macromolecules* **2002**, *35*, 2375.

Scheme 1



ties.²⁵ The maximum amount of POSS attached to polyimide, however, was no more than 2.5 mol %, because available polymer chain ends are limited. An increase in the number of covalently attached POSS is needed to further reduce the dielectric constant of polyimide.

In the present study, we adopt a new approach by using organic–inorganic nanocomposites with well-defined architectures to tether POSS molecules to the side groups of pre-synthesized polyimide to form nanoporous films. This approach can be an effective way to lower k while maintaining certain mechanical properties of the resulting nanocomposites. Additionally, we can have the advantage of producing materials with tunable dielectric constant by varying the molar ratio of POSS in polyimide. The nanocomposite films are easily processed using spin-coating techniques.

The synthesis of POSS/polyimide nanocomposites is shown in Scheme 1. Polyimide containing hydroxyl groups is obtained by reacting 3,3'-dihydroxy-4,4'-diaminobiphenyl (HAB) with 2,2'-bis(3,4-dicarboxyphenyl)hexafluoropropane dianhydride (6FDA) in *N,N*-dimethylacetamide, followed by a chemical imidization step. Then, the hydroxyl groups of the polyimide are reacted with chlorobenzyl cyclopentyl–POSS (Cl–POSS) molecules to form side-chain tethered structures. The morphologies of POSS/polyimide nanocomposites were

studied with X-ray diffraction, transmission electron microscopy, and scanning electron microscopy. The dielectric, thermal, and mechanical properties of the POSS/polyimide nanocomposites were also investigated.

Experimental Section

Materials. Chlorobenzylcyclopentyl–POSS (Cl–POSS) was obtained from Hybrid Plastics Company (Fountain Valley, CA). Electronic grade 3,3'-dihydroxy-4,4'-diaminobiphenyl (HAB) and 2,2'-bis(3,4-dicarboxyphenyl)hexafluoropropane dianhydride (6FDA) were purchased from Chriskev Co., Inc. THF was distilled under nitrogen from sodium benzophenone ketyl. *N,N*-Dimethylacetamide (DMAc) and xylenes were obtained from Aldrich (Milwaukee, WI).

Chlorobenzylcyclopentyl–POSS. ¹H NMR (300 MHz, THF-*d*8): 7.59 (d, $J = 7.5$ Hz, 2H), 7.33 (d, $J = 7.5$ Hz, 2H), 4.52 (s, 2H), 1.66–1.63 (m, 14H), 1.17–1.16 (m, 42H), 0.74–0.67 ppm (m, 7H). ²⁹Si NMR (600 MHz, THF): –67.8, –68.2, –79.6 ppm.

Hydroxyl Polyimide. Poly(amic acid) was synthesized by first putting 18.50 mmol of HAB into a three-necked flask containing 90.83 g of DMAc under nitrogen purge at 25 °C. After HAB was completely dissolved in DMAc, 18.88 mmol of 6FDA, which was divided into three batches, was added to the flask batch-by-batch with a time interval of 0.5 h between batches. When 6FDA was completely dissolved in DMAc, the solution was then stirred overnight under nitrogen to form the poly(amic acid) solution. The viscosity of the solution increased greatly during this period. Dry xylene (30 mL) was added to the flask, and the poly(amic acid) was imidized at 160 °C for 3 h. Water that was eliminated by the ring-closure reaction was separated as a xylene azeotrope at the same time. The resultant solution was added dropwise into an agitated solu-

(25) Leu, C. M.; Reddy, G. M.; Wei, K. H.; Shu, C. F. *Chem. Mater.* **2003**, *15*, 2261.

tion of methanol (500 mL) and 2 N HCl (10 mL) to obtain the brown hydroxyl polyimide. The polymer was redissolved in THF (50 mL) and further purified by reprecipitating into a solution of methanol (500 mL) and 2 N HCl (5 mL) from its THF solution. The polymer was then filtered and dried at 60 °C under vacuum for 24 h to afford 11.50 g of hydroxyl polyimide. ¹H NMR (300 MHz, THF-*d*₈): 10.06 (s, 2 H, OH), 8.10 (d, 2 H, *J* = 7.8 Hz), 7.95 (d, 2 H, *J* = 7.8 Hz), 7.90 (s, 2 H), 7.22 (d, 2 H, *J* = 7.8 Hz), 7.18 (s, 2 H), 7.14 ppm (d, 2 H). Molecular weight: *M*_w = 54 000, *M*_n = 15 000, with a polydispersity of 3.6.

Polyimide-Side-Chain Tethered POSS. NaH was used as a base to react with hydroxyl polyimide (2.00 g, 3.20 mmol) dissolved in DMAc and THF (15:15 mL) at room temperature. After the mixture was stirred for 1 h, various amounts of Cl-POSS (0.33 g, 0.320 mmol for the 10 mol % case) were added and then heated to 80 °C for 3 h. The feed molar ratios of Cl-POSS with respect to the equivalent of phenyl hydroxyl of polyimide were 10, 20, and 40 mol %. After filtration, the reaction mixture was slowly added to excess H₂O. The resultant powder was washed with MeOH and then dried in an oven.

POSS/polyimide nanocomposite films were prepared by dissolving the nanocomposite powder (1.00 g) in DMAc/THF cosolvent (5 mL/5 mL) and casting it on glass slides with a doctor blade, followed by drying in a vacuum at 50 °C for 24 h and then at 200 °C for 12 h. The resulting films were then peeled off of the glass slides as self-standing films for all mechanical and thermal evaluations.

Characterization. ¹H NMR spectra were recorded on a Varian Unity-300 NMR spectrometer. ²⁹Si NMR spectra were obtained from a DMX-600 NMR spectrometer. The molecular weights of hydroxyl polyimide were measured by gel permeation chromatography (GPC) using THF as the solvent. Polystyrene standards were used for calibration of GPC. An X-ray diffraction study of the sample was carried out using a MAC Science MXP18 X-ray diffractometer (40 kV, 200 mA) with copper target at a scanning rate of 4°/min. Thermal gravimetric and thermal transition analyses of polyimide films were carried out with a DuPont TGA 2950 and a DuPont DSC 2910 at a heating rate of 20 °C/min with nitrogen purge.

Samples for the transmission electron microscopy (TEM) study were prepared by first putting POSS/polyimide films into epoxy capsules and curing the epoxy at 70 °C for 12 h in a vacuum oven. Then the cured epoxy samples were microtomed with a Leica Ultracut Uct into ca. 90-nm-thick slices. Subsequently, a layer of carbon about 3 nm thick was deposited onto these slices, and the slices were placed on mesh 200 copper nets for TEM observation. The TEM instrument used was a JEOL-2000 FX, with an acceleration voltage of 200 kV. Scanning electron micrographs were obtained with a Hitachi-S-4700I microscope with an acceleration voltage of 10 kV.

The capacitance measurements for POSS/polyimide films were carried out in a sandwich structure (aluminum (Al)/polyimide/ITO glass). The top Al electrode, with an area of 1.0 mm², was deposited by thermal evaporation in a vacuum at 4 × 10⁻⁶ Pa on polyimide films, which were previously spun and dried on ITO glass. Then these films were dried at 130 °C under vacuum for 2 days. Film thicknesses were between 1.00 and 2.00 μm. SEM observation of the sandwich structure cross sections did not show any air gaps. Capacitances were determined with a HP4280A at a frequency of 1 MHz. The dielectric constants of the samples could then be calculated from their capacitances. The measured densities (*d*^M) of polyimide nanocomposite films were obtained by dividing the weight by the volume of the films. At least three specimens were used for each density data point. The relative porosity increase was calculated by eq 1

$$\text{Relative-porosity-increase } (\Phi_r) = \left[\frac{(d^T - d^M)}{d^T} \times 100\% \right] + (0.048 \times V\%) \quad (1)$$

↓
↓
 due to packing due to porosity core of POSS

where *d*^T is the theoretical density of the POSS/polyimide nanocomposites estimated from the weight percentage of POSS

Table 1. Content of POSS in POSS–Polyimide Nanocomposites

molar feed ratio of POSS (%)	elemental analysis			wt % of POSS in polyimide ^a (%)	mol % of POSS in polyimide ^b (%)	volume fraction of POSS ^c (%) (V%)
	C%	H%	N%			
0	57.2	3.4	4.9	0	0	0
10	56.6	4.0	4.2	14.3	10	17.5
20	54.3	4.6	3.6	26.5	22	31.5
40	51.9	4.8	3.1	36.7	35	42.5

^a The weight percentage (wt%) of POSS in polyimide was calculated from the elemental analysis results of pure polyimide and POSS–polyimide nanocomposites. ^b The content of POSS in polyimide with respect to the equivalent of phenyl hydroxyl of polyimide is calculated from the weight percentage (wt %) of POSS in polyimide. ^c The densities of POSS and polyimide are approximately 1.12 and .42 g/cm³, respectively.

in the nanocomposite and the density of POSS and polyimide (1.12 and 1.42 g/cm³). *V* % is the volume percentage of POSS in the nanocomposites. The nanoporosity core of POSS with a diameter of 0.54 nm in a POSS molecule of 1.5 nm in diameter represents only 4.8 volume% of the total POSS volume as provided by the hybrid plastics company.

Tensile properties of polyimide films were measured according to the specifications of ASTM D882-88 at a crosshead speed of 2 mm/min. The surface hardness values of polyimide films were measured in a nano-indentation experiment with a Berkovich indenter. The cross-section dimension of the base of the Berkovich indenter is 6 μm × 6 μm. The maximum applied load is 1000 μN, with loading and unloading times of 20 s, respectively; the waiting time was 5 s for the nano-indentation experiments.

Results and Discussion

Figure 1 shows ¹H NMR spectra of Cl-POSS, hydroxyl polyimide, and 35 mol % POSS/polyimide. The resonance peaks at 7.59 and 7.33 ppm are assigned to the aromatic protons (peaks a and b), and the resonance peak at 4.52 ppm is caused by the aliphatic proton (peak c). In Figure 1 (b), the peaks at 8.10, 7.95, and 7.90 ppm are assigned to the aromatic protons (4, 5, and 6) of the 6FDA moieties, and the peaks at 7.39, 7.21, and 7.18 ppm are attributed to the aromatic protons (1, 2, and 3) of the HAB moieties. For 35% POSS/polyimide, the three peaks at 7.61, 7.40, and 4.65 ppm result from the protons of the Cl-POSS moieties, indicating the presence of POSS molecules. The peaks for protons 1a, 2a, and 3a of the dihydroxybiphenyl moieties are shifted downfield to 7.2–7.3 ppm, implying the existence of covalently tethered POSS.

FTIR spectra of polyimide containing 35% POSS are given in Figure 2. The characteristic imide group bands at 1786 and 1725 cm⁻¹ imply a fully imidized structure, whereas the broad absorption around 3400 cm⁻¹ is attributed to hydroxy groups. The FTIR spectrum of 35% POSS–polyimide shows Si–O–Si asymmetric stretching absorptions between 1000 and 1180 cm⁻¹ and the aliphatic C–H stretching band between 2800 and 2900 cm⁻¹, confirming that POSS molecules are tethered to polyimide. The ²⁹Si NMR spectra shown in Figure 2 (b) provide direct evidence that the silsesquioxane cages remain intact following the reaction.

Table 1 presents the elemental analysis results of hydroxyl polyimide and POSS–polyimide nanocomposites. The weight % of POSS molecules tethered to the side chain is determined from the elemental analysis, and the volume percentage of POSS in polyimide is

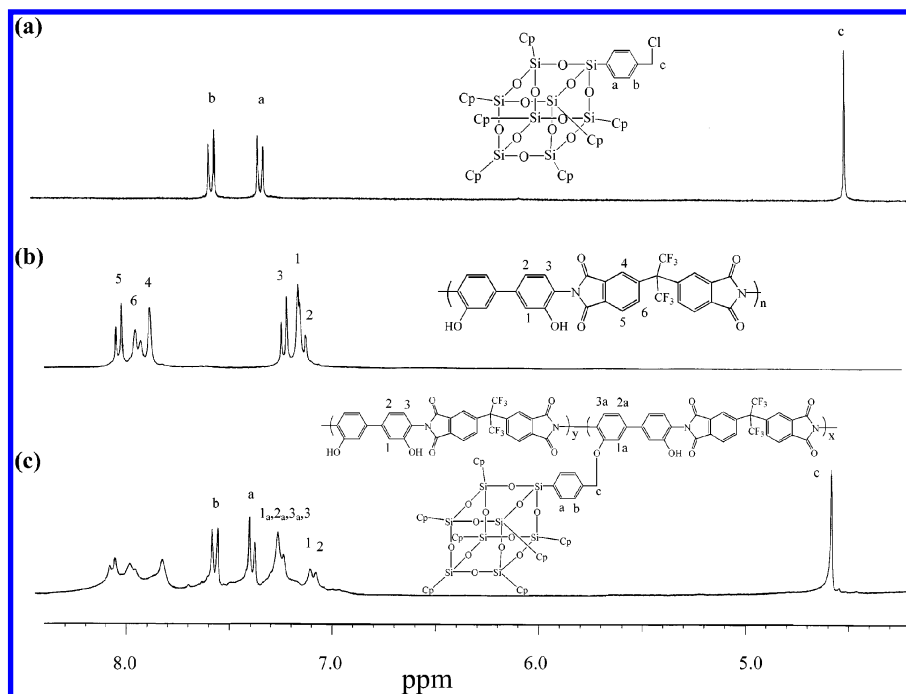


Figure 1. ^1H NMR spectra of (a) Cl-POSS, (b) hydroxyl polyimide, and (c) 35% POSS-polyimide.

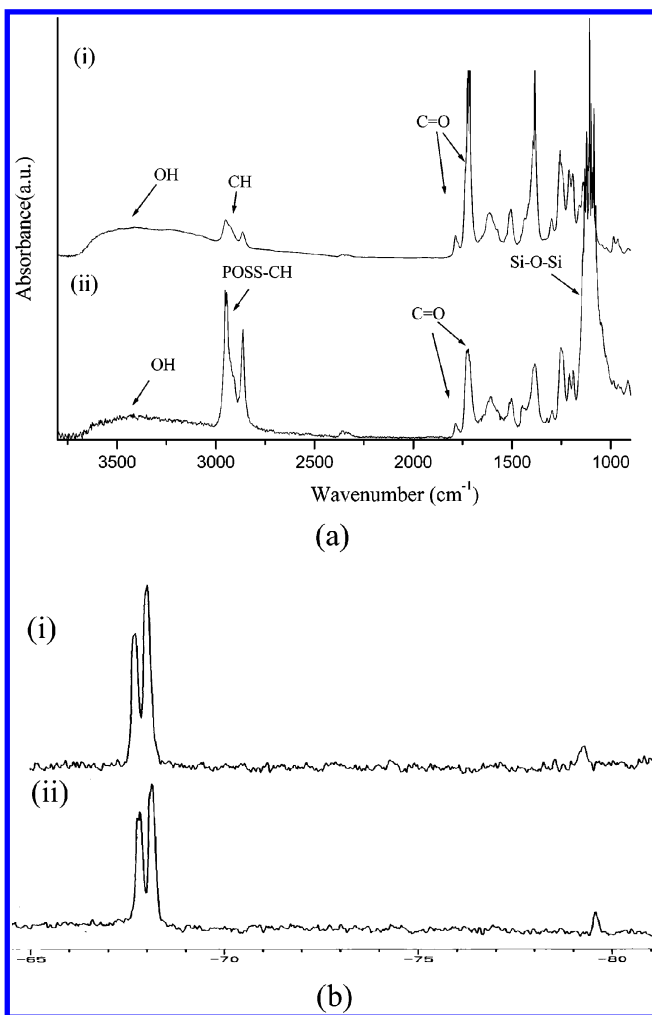


Figure 2. (a) FTIR spectra of (i) hydroxyl polyimide and (ii) 35% POSS-polyimide. (b) ^{29}Si NMR spectra of (i) Cl-POSS and (ii) 35% POSS-polyimide.

calculated from the densities of POSS and polyimide²⁶ (1.12 and 1.42 g/cm³, respectively).

Figure 3 (a) shows wide-angle X-ray diffraction (WAXD) curves of the POSS-polyimide nanocomposite films. There are five distinct diffraction peaks at $2\theta = 8.3, 11.3, 12.0, 19.1,$ and 25.9° by Cl-POSS, corresponding to d -spacings of 10.5, 7.2, 6.9, 4.6, and 3.3 Å, respectively. The peak corresponding to a d -spacing of 10.5 Å is caused by the size of Cl-POSS molecules; the remaining peaks are produced by the rhombohedral crystal structure of POSS molecules.²⁴ No X-ray diffraction peak is obtained for pure polyimide. POSS-polyimide nanocomposites having different molar ratios exhibit four distinct X-ray diffraction peaks (with d -spacings of 10.5, 7.2, 6.9, and 4.6 Å) that were also found in the case of Cl-POSS. This indicates that the amorphous polyimides, which POSS molecules are tethered to, do not disrupt the formation of POSS crystalline aggregates. When the POSS content increases to 35 mol %, the intensities of the POSS peaks become stronger and two new peaks corresponding to d -spacings of 4.1 and 3.7 Å emerge. This suggests that the crystallite structure of tethered POSS is slightly different from that of Cl-POSS. Figure 3 (b) shows the transmission electron micrograph of a cross-section of the 35 mol % POSS-polyimide film. It displays clusters of 10-nm size by tethered POSS distributed in the polyimide matrix.

Figure 4 (a), (b), and (c) show the morphologies of the fractured surfaces of POSS-polyimide nanocomposites obtained by field-emission scanning electron microscopy. In Figure 4 (a), the 10 mol % case, the fractured points seem to occur along the tethered POSS crystalline aggregates, which are seen as gray spots in the dark background. The distribution of these fractured points is roughly uniform. In Figure 4 (b), the fractured points appear to contain more gray spherical particles (about 10 nm in size) for the 22 mol % POSS-polyimide case. In Figure 4 (c), which is the 35 mol % POSS-polyimide case, the 10-nm gray particles are more widely distrib-

Table 2. Capacitance, Dielectric Constant, and Densities of POSS–Polyimide Nanocomposites

mol % of POSS in polyimide	capacitance ($\times 10^{11}$) (at 1 MHz)	dielectric constant (at 1 MHz)	theoretical density ^a (d_T) (g/cm ³)	measured density (d_M) (g/cm ³)	relative-porosity-increase (ϕ_r) (%)
0	2.35 \pm 0.19	3.35 \pm 0.16	1.42	1.42 \pm 0.04	0
10	1.91 \pm 0.09	2.83 \pm 0.04	1.37	1.30 \pm 0.04	5.9
22	1.14 \pm 0.08	2.67 \pm 0.07	1.33	1.19 \pm 0.07	12.0
35	1.64 \pm 0.12	2.40 \pm 0.04	1.29	1.12 \pm 0.01	15.2

^a Theoretical density (d_T): estimated from the weight percentage of POSS in the nanocomposite and the density of POSS and polyimide (1.12 and 1.42 g/cm³).

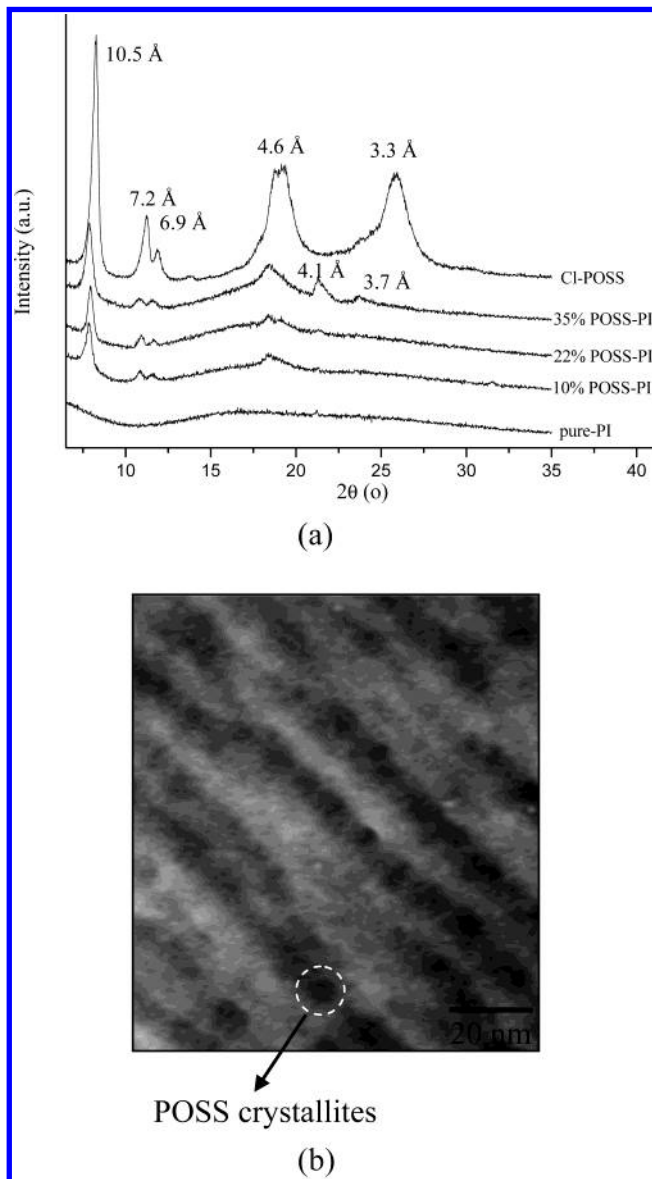


Figure 3. (a) X-ray diffraction curves of POSS/polyimide nanocomposite films. (b) Transmission electron micrograph of a cross section of POSS–polyimide nanocomposite film.

uted and appear to form an ordered structure; this conclusion is supported by two new peaks in the wide-angle X-ray results. The transmission electron micrograph of a cross-section of the 35 mol % POSS–polyimide film reveals a layer-by-layer structure that also supports the formation of an ordered architecture by POSS crystallites in the polyimide, as shown in Figure 4 (d). Here, the layers consist of POSS crystallite aggregates with an average layer thickness of 10 nm. The ordered structure is most likely caused by the phase-separation of POSS crystallites from polyimide, as polar–polar interactions (O=C–N) between imide

segments are quite different from van der Waals interactions between the cyclopentyl groups of POSS molecules. A schematic drawing of the architecture of polyimide-tethered POSS is given in Figure 5, where the average length of polyimide molecules is more than 50 nm, as converted from its molecular weight ($M_w = 54\,000$).

Table 2 presents the capacitance, dielectric constants, and densities of the POSS–polyimide nanocomposites. The dielectric constant of the POSS–polyimide nanocomposites decreases, and the relative-porosity-increase increases, as the amount of POSS increases. The maximum reduction in the dielectric constant of the POSS–polyimide nanocomposites is about 28%, by comparing 35 mol % POSS–polyimide to pure polyimide ($k = 2.40$ vs 3.35). There are a few possible causes for the reduction in the dielectric constant. Because the porosities of these nanocomposite films are difficult to obtain, we adopt a simple measure to compare the relative porosities of these films. The relative-porosity-increase (ϕ_r) is defined as the increased external porosity due to the incorporation of POSS molecules in polyimide, excluding the nanoporosity of POSS molecules themselves, and is calculated by eq 1 in the characterization section. The ϕ_r for the 35 mol % POSS–polyimide case is 15.1%, and this ϕ_r value cannot possibly account for all the 28% reduction in the dielectric constant of the nanocomposite film. Hence, the reduction is most likely due to the nanoporosity in the core of the POSS molecules¹⁰ and the external porosity introduced by tethering POSS to the polyimide side chains, as evidenced by the decreasing density and the increasing ϕ_r of the nanocomposite films when the amount of POSS present in the film increases. The increase in the external porosity in the nanocomposites as a result of POSS molecules in turn can be further interpreted as an increase in the free volume of the nanocomposites because of the interaction of polyimide segments and tethered POSS. This also means that the free volume for polyimide in the nanocomposites increases with the amount of the tethered POSS. The increase in the free volume of polyimide corresponds quite well to the fact that the glass transition temperature (T_g) of the polyimide in the nanocomposites is lower than that of the pure polyimide.²⁷ Another possible contribution to the lower dielectric constant comes from the fact that the hydroxyl groups on polyimide are partly replaced by POSS molecules, leading to a decrease in the polarity or capacitance of the nanocomposite; this effect is limited, however.

Degradation temperatures (T_d) of POSS–polyimide nanocomposites are lower than that of pure polyimide,

(27) Merkel, T. C.; Freeman, B. D.; Spontak, R. J.; He, Z.; Pinnau, I.; Meakin, P.; Hill, A. *Science* **2002**, *296*, 519.

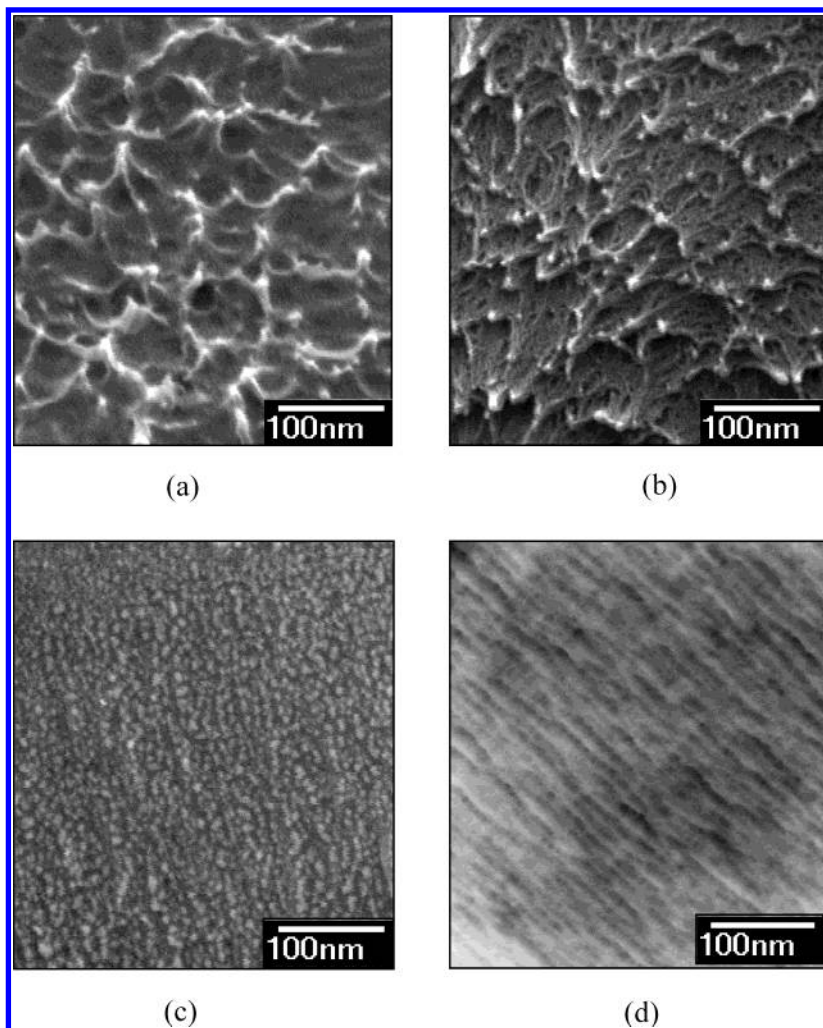


Figure 4. Field-emission scanning electron micrographs of the fractured surface of (a) 10 mol %, (b) 22 mol %, and (c) 35 mol % POSS–polyimide nanocomposites. (d) Transmission electron micrograph of a cross section of a 35 mol % POSS–polyimide nanocomposite film.

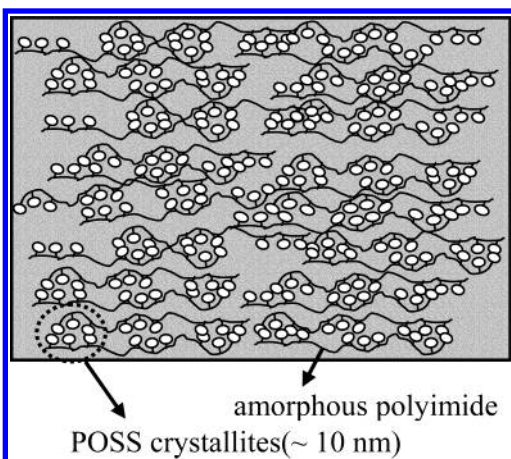


Figure 5. Schematic drawing of the architecture of polyimide-tethered POSS.

resulting from the degradation of POSS molecules (at ~ 400 °C). Table 3 shows a slight reduction in the Young's modulus for the 10 mol % POSS–polyimide case, as compared to that of pure polyimide, owing to POSS aggregates. In addition, the maximum stress decreases more appreciably. As the amount of POSS increases to 22 and 35 mol %, the decrease in the Young's modulus and the maximum stress become

Table 3. Thermal and Mechanical Properties and Surface Hardness of POSS–Polyimide Nanocomposites

mol % of POSS in polyimide	T_g^a (°C)	T_d^b (°C)	Young's modulus (GPa)	max stress (MPa)	surface hardness (GPa)
0	359.3	430.2	1.86 ± 0.08	59.2 ± 7.7	0.15 ± 0.01
10	355.1	415.1	1.85 ± 0.09	45.1 ± 5.1	0.11 ± 0.02
22	350.5	407.9	1.20 ± 0.02	22.3 ± 4.9	0.07 ± 0.01
35	337.6	405.7	0.61 ± 0.07	11.2 ± 3.9	0.06 ± 0.02

^a T_g : glass transition temperature. ^b T_d : thermal degradation temperature at 5 wt % loss.

rather prominent, a result of weakened interactions between polyimide in the presence of POSS. The surface hardness of the nanocomposite films coated on glass, shown in Table 3, also decreases with an increasing amount of POSS because of the increased free volume.

Concluding Remarks

Nanoporous organic–inorganic nanocomposites were prepared by tethering POSS molecules to the side groups of pre-synthesized polyimide. The dielectric constants of the resultant nanocomposites are lower due to the increased free volume and less polar POSS molecules, and can be tuned by varying the molar ratio of POSS; polyimide molecules offer additional advan-

tages of maintaining certain thermal and mechanical strengths. POSS molecules tethered to the side groups of polyimide retain a crystallized structure, but form an additional ordered architecture as the mole ratio of POSS increases to 35%.

Acknowledgment. We appreciate the financial support provided by the National Science Council through project NSC 91-2120-M-009-001.

CM030393B